Proceedings of the 8th International Conference on Civil Engineering for Sustainable Development (ICCESD 2026), 5~7 February 2026, KUET, Khulna, Bangladesh

COST-EFFECTIVE SEISMIC RETROFITTING OF INTERIOR BEAM-COLUMN JOINTS: A NUMERICAL INVESTIGATION OF CFRP AND TRM

Sithi Roy[1], Ankon Roy[2], Md. Shoriful Islam[3], Md. Imran Hossain[4], Jobaer Hossain[5] and Tahmina Tasnim Nahar[*6]

[1] *Undergraduate Student, Pabna University of Science and Technology, Bangladesh, e-mail: sithiroy201140@gmail.com*
[2] *Undergraduate Student, Pabna University of Science and Technology, Bangladesh, e-mail: ankonroy2515@gmail.com*
[3] *Graduate Student, Pabna University of Science and Technology, Bangladesh, e-mail: shorifulshohag19@gmail.com*
[4] *Graduate Student, Pabna University of Science and Technology, Bangladesh, e-mail: imranhossainimran695@gmail.com*
[5] *Graduate Student, Pabna University of Science and Technology, Bangladesh, e-mail: jobaer3686@gmail.com*
[6] *Professor, Pabna University of Science and Technology, Bangladesh, e-mail: tasnim@pust.ac.bd*

***Corresponding Author**

ABSTRACT

Beam-column joints play a crucial role in the overall performance of a building during an earthquake, and they form an internal contributor to the collapse of the building. Retrofitting of beam-column joints is, therefore, an important step in improving the seismic performance of existing buildings that were not designed or constructed to withstand seismic forces. This study presents a nonlinear Finite Element Analysis (FEA) to investigate the comparative hysteresis behavior of textile-reinforced mortar (TRM) and carbon fibre-reinforced polymer (CFRP) retrofitted reinforced concrete interior beam-column joint specimens. A parametric study was conducted on a control specimen and four retrofitted configurations (one, two, and three layers of TRM and a single layer of CFRP) using the Concrete Damage Plasticity (CDP) model. The designed specimens were analysed under a constant axial load and reversed quasi-static cyclic load, where 400 kN load was applied at the top of the column part (axial pressure load), and the reversed cyclic load was applied at the end of the beam part. Finally, the numerical predictions indicate that the peak load in the positive direction of the retrofitted specimen over that of the control specimen was improved by 12.5% with one layer of TRM, 24.95% with two layers of TRM, 32% with three layers of TRM, and 20.5% with a single layer of CFRP. In the negative direction, it was improved by 7.35% with one layer of TRM, 20.61% with two layers of TRM, 31.2% with three layers of TRM, and 14.35% with a single layer of CFRP. In terms of cost analysis, the result showed that even after adding two or three layers of TRM, the total cost remained lower than that of a single layer of CFRP. Although a single layer of CFRP provided more strength than TRM (one layer), it was less strong than two or three layers of TRM. So it could be decided from this study that TRM was a more economical retrofit technique than CFRP.

Keywords: *Interior Beam-Column Joints, Reversed Cyclic Load, Textile-Reinforced Mortar, Carbon Fibre-Reinforced Polymer, and Cost Analysis.*

1. INTRODUCTION

Reinforced Cement Concrete (RCC) frame structures constitute the backbone of global infrastructure due to their durability and economic viability. However, over time, many RCC-framed buildings become less safe and less useful because of changes in use, design requirements, loading conditions, and natural disasters like earthquakes. A significant portion of the existing building stock was constructed prior to the implementation of modern seismic design codes (Said and Nehdi 2004). In RCC structures, the beam-column joint represents the most critical region, acting as the pivot for force transfer between structural members. During seismic events, the joints experience complex shear and flexural stresses. Older buildings frequently lack the necessary steel ties within their joints, making these connections the weakest part of the frame. This might result in brittle failure and possibly catastrophic structural collapse (Kaliluthin, Kothandaraman, and Suhail Ahamed 2014). Recent seismic disasters like the 2023 Turkey–Syria earthquake have highlighted the dangers of joint deficiencies and the immediate necessity of implementing strengthening measures to ensure public safety.

To mitigate these risks, seismic retrofitting using externally bonded reinforcement has become standard practice. Common strategies include steel jacketing, concrete jacketing, wrapping with fiber-reinforced polymer (FRP) sheets, Textile Reinforced Mortar (TRM), external pre-stressing, etc. at the member level. Among the available techniques, Carbon Fiber Reinforced Polymer (CFRP) is widely regarded as the most effective solution due to its exceptional tensile strength, corrosion resistance, and high stiffness-to-weight ratio. Extensive research confirms that wrapping joints with CFRP sheets can significantly restore shear capacity and ductility (Golias and Karayannis 2025; Kim, Choi, and Kim 2025; Vijayan et al. 2023). However, despite its structural dominance, CFRP presents distinct practical and economic limitations. CFRP has a relatively high cost and requires specialized installation techniques. Its performance drops under high temperatures, and its vulnerability to moisture is a significant drawback (Pan, Xian, and Silva 2015; Shrestha, Zhang, and Ueda 2016; Vijayan et al. 2023; Yin et al. 2025).

These drawbacks have driven the search for more sustainable and compatible alternatives, leading to the emergence of Textile Reinforced Mortar (TRM). Unlike FRP systems, TRM embeds high-strength fiber textiles like carbon, basalt, glass, or aramid within an inorganic cementitious mortar matrix. This sustainable alternative to FRP systems is ideal for severe or highly humid environments due to its inorganic matrix's compatibility with concrete and masonry, high vapor permeability, and temperature tolerance. Studies show that basalt-based TRM can increase the shear strength of reinforced concrete beams by 36% to 88% (Al-Salloum et al. 2012; Triantafillou et al. 2006). Also, TRM was found as an effective seismic retrofit that confines concrete and reduces cracking during earthquakes. Tests show that one U-wrapped layer can reach a stress of 491 MPa at 2.18% strain, while using high-strength mortar further boosts the bond and shear capacity (Ghobarah and Said 2002; Tetta, Koutas, and Bournas 2015). There remains a lack of comprehensive research that directly compares the structural efficiency of TRM against the industry-standard CFRP, specifically for interior beam-column joints using advanced numerical modeling.

Moreover, a significant gap exists in the economic evaluation of these retrofitting techniques. Most studies focus solely on structural gains without addressing the cost-benefit ratio, which is a decisive factor for engineers and stakeholders in developing nations. It is crucial to determine not just which material is stronger, but which offers the most sustainable balance between performance and cost. Without this comparative data, engineers struggle to justify switching from the proven CFRP method to the more sustainable TRM alternative.

However, conducting full-scale experimental tests for multiple retrofitting configurations is often resource-intensive and time-consuming. Therefore, this research utilizes nonlinear Finite Element Analysis (FEA) as a predictive comparative tool. The primary objective is to evaluate the relative structural efficiency and economic feasibility of TRM compared to CFRP using established constitutive material models. By simulating the internal stress transfer mechanisms and analyzing the cost-benefit ratio, this theoretical framework serves as a vital preliminary assessment to identify optimal retrofitting strategies before large-scale experimental implementation.

2. METHODOLOGY

The behavior of beam-column connections subjected to cyclic load was analyzed using a finite element model created with ABAQUS software. T3D2, C38DR, S4R, and B31 elements were used to simulate the beam-column junctions. The characteristics of the various components employed in the investigated model are described below.

2.1 Constitutive Modeling Framework

To ensure the theoretical reliability of the numerical predictions, this study utilized the Concrete Damage Plasticity (CDP) model in ABAQUS. The geometry and reinforcement detailing of the reference specimen were adopted from the standard literature to represent a typical non-ductile joint (Ghobarah and Said 2002).

The compressive behavior of concrete was modeled using the stress-strain relationship proposed by Saenz (1964), while the tensile behavior, including tension stiffening, was defined according to Hillerborg's (1976) fracture energy criterion. This approach allows the model to accurately simulate the formation of diagonal shear cracks and the subsequent degradation of stiffness under cyclic loading.

2.2 Modeling of Retrofitting Interfaces

A critical aspect of this comparative study is the interface modeling between the concrete substrate and the retrofitting layers. The bond between the CFRP sheet and concrete was modeled using a cohesive zone model. This captures the linear-elastic nature of the epoxy resin and simulates potential debonding failure, consistent with the study of (Tetta et al. 2015)

The TRM composite was modified by a friction coefficient to account for the mechanical interlock of the textile grid. This methodology aligns with the confinement principles described in the study of (Triantafillou et al. 2006).

2.3 Geometry Modeling of Beam-column Joint

The foundational geometry comprised an interior joint of a reinforced concrete frame. The column measured 400 mm × 400 mm in cross-section, intersected centrally by a beam of 400 mm width and 500 mm depth. The beam extended 1950 mm from either connection face, and the specimen reached a total height of 3236 mm. For the column, longitudinal reinforcement bars were selected at 5/8 inch diameter, accompanied by 3/8 inch tie bars for transverse confinement. Double tie bars were positioned at 85 mm spacing close to the beam-column interface, while single tie bars at 150 mm intervals covered the remainder of the column (Allam, Elbakry, and Arab 2018).

In the beam, shear reinforcement mirrored the column's bar specifications, with double stirrups arranged at 100 mm spacing near the support region and wider spacing further out. Top and bottom longitudinal bars, each 5/8 inch in diameter, provided essential flexural strength. These reinforcement arrangements are illustrated in Figure 1 and Figure 2, and all geometric parameters are collated in Table 1 (Ghobarah and Said 2002; Pauline et al. 2022).

Table 1: Geometric properties of beam and column

Part	Parameter	Value
Column part	Longitudinal steel diameter(mm)	15.872
	Transverse steel diameter(mm)	9.525
Beam part	Width (mm)	400
	Depth (mm)	500
	Effective depth(mm)	440
	Slab thickness (mm)	100
	Top steel diameter(mm)	15.875
	Top steel ratio	0.009
	Bottom steel diameter (mm)	15.875
	Bottom steel Ratio	0.009
	Transverse steel diameter (mm)	9.525

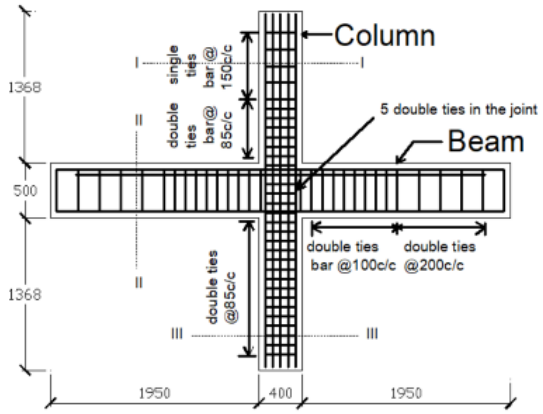

Figure 1: Reinforcement planning of beam-column joint (all dimensions in mm).

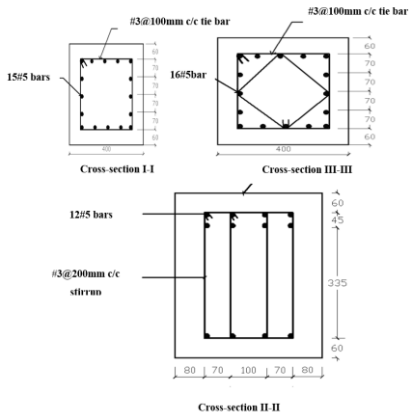

Figure 2: Cross-section of beam and column portion (all dimensions in mm).

2.4 Materials Modeling

2.4.1 Concrete

To realistically address the nonlinear response of concrete, particularly under cyclic loading, the Concrete Damage Plasticity (CDP) model**,** designed by Williams and Warnke was implemented in ABAQUS. This approach captures both cracking and crushing effects, using nonlinear stress-strain curves to simulate how concrete weakens and deforms under different loads. The formula according to the model is as follows:

$$f_c = f'_c\left[\frac{2\varepsilon_c}{\varepsilon_{co}} - \left(\frac{\varepsilon_c}{\varepsilon_{co}}\right)^2\right] \quad where\ 0 \le \varepsilon_c \le \varepsilon_{co} \tag{1}$$

$$f_c = f'_c\left[\frac{0.15f'_c}{\varepsilon_c - \varepsilon_{co}}\right](\varepsilon_c - \varepsilon_{co}) \quad where\ \varepsilon_c > \varepsilon_{co} \tag{2}$$

$$\varepsilon_{co} = \frac{2f'_c}{E_c} \tag{3}$$

$$f_t = 0.62\sqrt{f'_c} \tag{4}$$

Where, f_c = concrete compressive stress (MPa), ε_c = strain corresponding to f_c, f'_c = concrete compressive strength (MPa), ε_{co} = strain at peak compressive strength, E_c = modulus of elasticity of concrete and f_t = tensile strength of concrete.

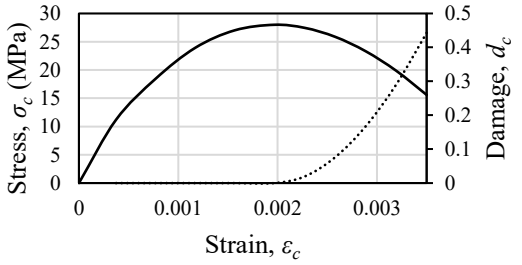

(a)

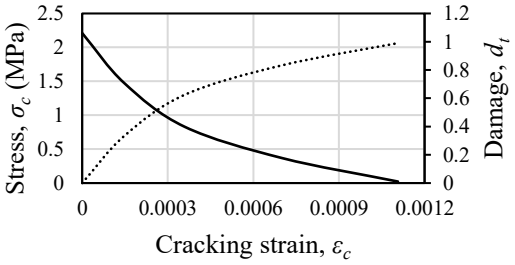

(b)

Figure 3: (a) Compresive crushing behavior, (b) Tensile softening behavior.

To model the concrete, a general-purpose 8-node linear brick element known as a C3D8R type element is used. Concrete is modeled as a composite using CDP (Concrete Damage Plasticity) in ABAQUS, which is shown in Figure 3.

2.4.2 Steel Reinforcement

Steel rebar is assumed linearly elastic, with the elastic modulus range 200-210 GPa and Poisson's ratio 0.28-0.3. To ensure such a perfect link assumption, the surrounding steel nodes and concrete nodes are merged. This approach allows discrete modeling of steel reinforcement, where each bar is independently simulated using the T3D2 element, a 3-D spar truss element that is an unaxial tension-compression element defined by two nodes with three translational degrees of freedom at each node and with plastic bending capability. Material properties of steel used are given in Table 2.

Table 2: Material Properties of steel

Parameter	Properties
Density	7783 kg/m^3
Average yield strength of longitudinal steel, f_y	500 MPa
Average yield strength of transverse steel, f_y	380 MPa
Average yield strength of mild steel	260 MPa

2.4.3 Textile Reinforced Mortar (TRM) Materials

TRM is modeled using S4R shell elements in the finite element analysis. The system consists of mesh textiles (typically in orthogonal orientations) embedded in an inorganic mortar matrix. The TRM wrap fully covers the column up to 550 mm past the beam face, with U-shaped jackets provided on the joint and beam, each extending 800 mm from the column face. The slab has a thickness of 100 mm, which prevents TRM placement on the top beam face. Figure 4 shows the finite element modeling of TRM .

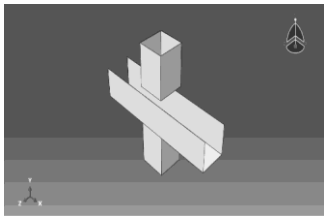

Figure 4: Finite element modeling of TRM.

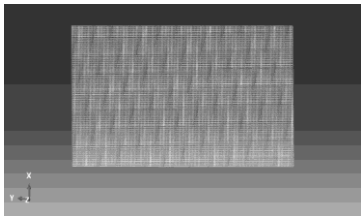

Figure 5: Design of textile sheet.

Reinforcement within the TRM is represented using B31 beam elements for fibers, with each textile layer having a thickness of 0.147 mm. The gap between layers is 10 mm to ensure even matrix penetration and bonding. This composite design enhances mechanical interlock and increases shear and tensile strength for structural strengthening. The space between the two layers is 10 mm, which is shown in Figure 5.

2.4.4 Mortar

In TRM, mortar serves to bind fibers, protects them against environmental damage, and distributes loads evenly across the fibers. The thickness of the mortar layer is 2 mm. To model the mortar, a general-purpose 8-node linear brick element known as a C3D8R type element is used, which is shown in Figure 6.

Figure 6: Finite element of mortar shell.

The material properties of TRM are given in Table 3.

Table 3: Material properties of TRM

Property Category	Property	Value	Units	Notes
Elastic Moduli	E_X	82.5	Gpa	
	E_Y	4.6	Gpa	
	E_Z	4.6	GPa	
Major Poisson Ratio	V_{XY}	0.22	-	Dimensionless
	V_{XZ}	0.22	-	Dimensionless
	V_{YZ}	0.33	-	Dimensionless
Shear Modulus	G_{XY}	1500	MPa	
	G_{XZ}	1000	MPa	
	G_{YZ}	1000	MPa	
Mechanical Strength	Yield stress	200	MPa	
	Fracture strain	0.95	%	
Physical/Geometric	Thickness	0.147	mm	Eq. fiber thickness without mortar
	Mass density	1.95		

2.4.5 Carbon Fiber Reinforced Polymer (CFRP)

Carbon fiber-reinforced polymer (CFRP) was implemented in ABAQUS based on a two-part system: polymer and epoxy resin, with the resin serving as a strong binder. A two-component epoxy matrix was specified for externally bonding CFRP sheets onto concrete surfaces (Wang et al. 2017). CFRP acted as a wrapping material in this design, using S4R shell elements, consistent with the element types applied in TRM modeling. The properties of CFRP are given in Table 4.

Table 4: Material properties of CFRP

Property Category	Property	Value	Units
Elastic Moduli	E_X	77.3	Gpa
	E_Y	4.6	Gpa
	E_Z	4.6	GPa
Major Poisson Ratio	V_{XY}	0.22	-
	V_{XZ}	0.22	-
	V_{YZ}	0.33	-
Shear Modulus	G_{XY}	3270	MPa
	G_{XZ}	3270	MPa
	G_{YZ}	1680	MPa
Mechanical Strength	Tensile	777	MPa
Physical/Geometric	Thickness	1	mm

2.5 Meshing

Due to improved sampling of the designs throughout the physical domains, the solution is often more

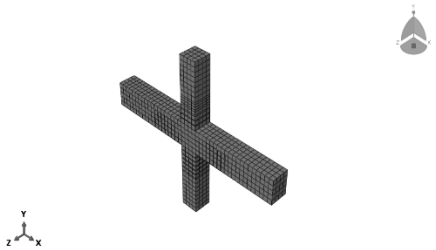

Figure 7: Meshing in Beam-Column Joint.

accurate the smaller the mesh size. The models are mashed up part by part but assembled independently with three different types of element shapes: line, hexahedral, and quadrilateral. The approximate global size of the elements was taken as 100 mm. Some portions of the model were being tweaked to provide accurate element shapes. The following Figure 7, shows the model after assigning mesh to all parts.

2.6 Loading Strategy and Boundary Condition

The designed beam-column joint was analyzed under a constant axial load and reversed quasi-static cyclic load, where a 400 kN load was applied at the top of the column part as pressure load and the cyclic load was applied at the end of the beam part. The cyclic loading history is shown in Figure 8. Two equal opposite parallel forces were also applied at both ends of the beam to resist the couple moment formed along the beam portion due to the external force, which is shown in Figure 9. Roller support is provided at the top of the column face with a restricted horizontal displacement Ux. The bottom face of the column acts as a fixed support where no specific movement and rotation take place (Ux = Uy = Uz = 0, URx = URy = URz = 0). The boundary condition is shown in Figure 9.

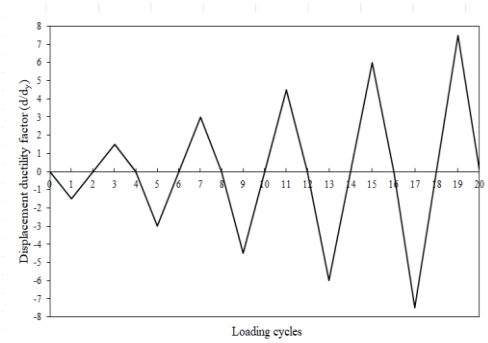

Figure 8: History of cyclic load.

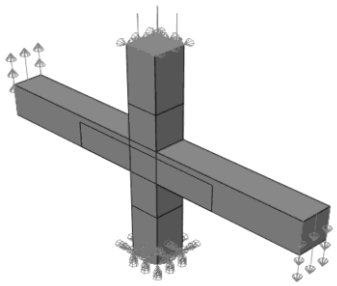

Figure 9: Loading and boundary condition.

2.7 Test Specimen

To find out the effectiveness of TRM according to strength and cost analysis, five types of specimens were analyzed under a preselected cyclic load, which is described below.

2.7.1 SP- 1: Unretrofitted Beam-column Joint

The specimen was subjected same axial load and cyclic load which was used in the case of retrofitted beam-column joint. The model of unretrofitted beam-column joint is shown in Figure 10.

2.7.2 SP-2: Retrofitted Beam-column Joint with One Layer of CFRP

For SP-2, a single layer of CFRP sheet was used to retrofit the beam-column joint. The column was fully wrapped in CFRP, while the beam received a U-shaped wrap at the joint area. The retrofitting involved establishing a surface-to-surface contact constraint in ABAQUS, where the concrete at the

joint acted as the master surface, and the CFRP sheet served as the slave surface. Cohesive behavior for the contact interaction was enabled to ensure adequate bonding between the CFRP and the concrete (Figure 11).

2.7.3 SP-3: Retrofitted Beam-column Joint with One Layer of TRM

A single layer of TRM was applied to the control specimen, embedding textile in a 2 mm mortar matrix. Surface-to-surface contact was employed as a sort of constraint to join the two components; the concrete of BCJ served as the master surface, and the TRM surface as the slave surface. The beam-column joint received a U-shaped wrap, as for CFRP (Figure 12). The TRM layer increased the beam depth from 440 mm to 442 mm.

2.7.4 SP-4: Retrofitted Beam-column Joint with Two Layers of TRM

One layer of TRM was again wrapped around the previously strengthened specimen (SP-3). For connecting surface, the previous TRM layer served as a master surface whereas the new one served as the slave surface. Then the total layer thickness was 4 mm, and the beam effective depth transferred from 440 mm to 444 mm (Figure 13).

2.7.5 SP-5: Retrofitted Beam-column Joint with Three Layers of TRM

To increase the strength of the specimen, one layer of TRM was further added to the previous (SP-4). For connecting surface to surface constraint the previous procedure was followed and the effective depth of the beam was increased from 440 mm (control specimen) to 446 mm (Figure 14).

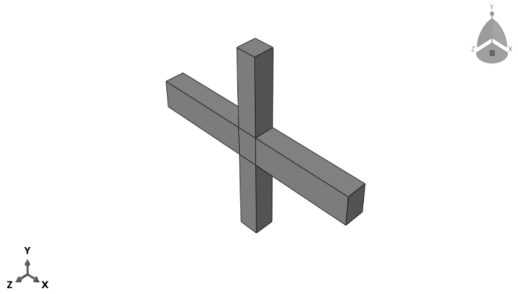

Figure 10: Unretrofitted beam-column joint.

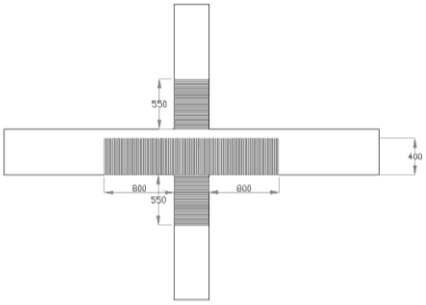

Figure 11: Retrofitted beam-column joint with one layer of CFRP.

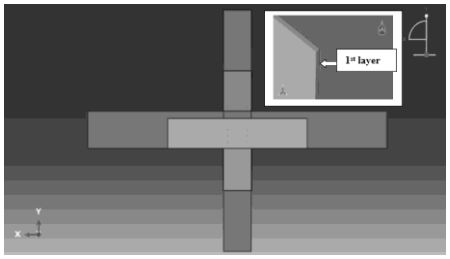

Figure 12: Retrofitted beam-column joint with one layer of TRM.

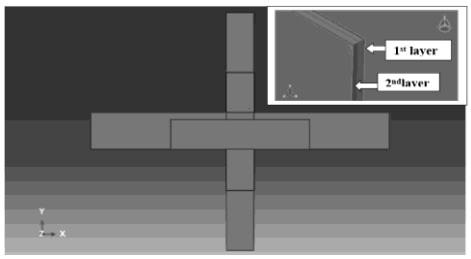

Figure 13: Retrofitted beam-column joint with two layers of TRM.

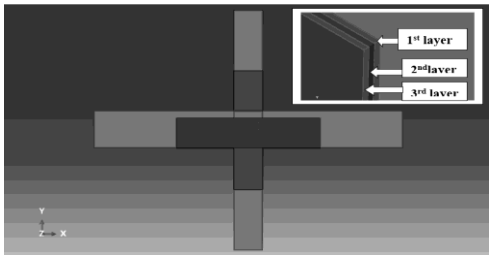

Figure 14: Retrofitted beam-column joint with three layers of TRM.

3. RESULTS AND DISCUSSIONS

3.1 Hysteretic Response and Damage Mechanism

Hysteresis curves illustrate structural performance under reversed cyclic loads like earthquakes or wind. Full hysteresis loops have loading and unloading curves. After the members have yielded, the loading curve's slope decreases with increasing displacement and repeated loading reduces structural flexibility. The unloading curve's slope likewise decreases with cycles, indicating stiffness loss. With additional cycles, residual deformation grows despite unloading. These curves show yield, ultimate loading capacity and energy dissipation of the structure subjected to reversed cyclic loading. Cyclic loading damages members more with each cycle and displacement amplitude increase. Finite element models can forecast beam-column junction behavior better than current approaches, which struggle to calculate the skeleton curve or capture mechanical property degradation.

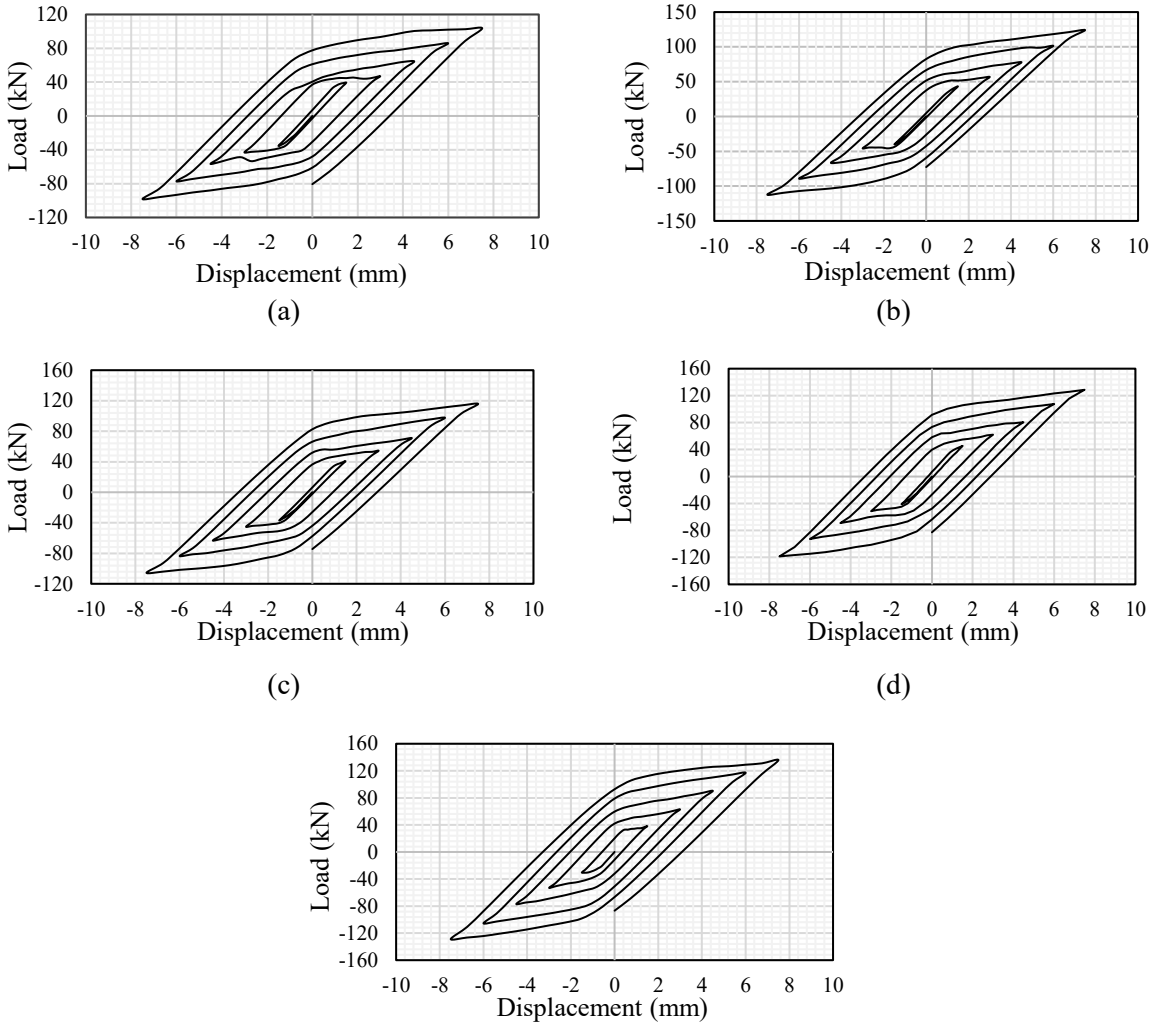

Figure 15: Hysteresis curve of specimen, (a) SP-1, (b) SP-2, (c) SP-3, (d) SP-4, (e) SP-5.

The seismic performance of the joints was evaluated through the numerically generated cyclic load-displacement hysteresis loops (Figure *15*). The shape of the hysteresis loops indicates low energy dissipation capacity in case of SP-1 (unretrofitted), as shown in [Figure *15*(a)]. This may be due to the lack of transverse reinforcement, which leads to the rapid opening and closing of diagonal shear cracks, causing significant slippage of the longitudinal bars and loss of aggregate interlock (Kaliluthin et al. 2014). The limited peak loads of 103 kN in positive direction and 98.2 kN in negative direction confirm

that the joint failed in a brittle shear mode before flexural yielding could develop. A single-layer CFRP specimen (SP-2) showed a stable response with peak loads of 124.11 kN and 112.3 kN in positive and negative direction respectively [Figure *15*(b)], owing to the high elastic modulus of carbon fibers which effectively confines the joint core and restricts lateral concrete dilation (Golias and Karayannis 2025). However, the post-peak stiffness degradation was abrupt. This is because epoxy-bonded systems behave in a linear-elastic manner, leading to sudden debonding failure without the gradual softening capability inherent in cementitious composites (Tetta et al. 2015). As illustrated in Figure *15*(c), Figure *15*(d), and Figure 15(e) respectively, the specimens retrofitted with one to three layers of TRM (SP-3, SP-4, and SP-5) showed a ductile response with visibly wider hysteresis loops. A clear correlation was observed between the number of layers and strength. peak positive loads rose from 115.87 kN in SP-3 to 135.97 kN in SP-5. Similarly, negative peak loads increased from 105.57 kN to 128.87 kN, which confirms the effectiveness of multi-layer TRM strengthening. The single-layer TRM (SP-3) achieved a lower peak (115.87 kN) than CFRP because the inorganic mortar matrix allows for microscopic "telescopic" slippage of the fiber rovings, which reduces initial stiffness but promotes ductility (Al-Salloum et al. 2012). Importantly, the multi-layer specimens (SP-4 and SP-5) showed non-linear improvement. The dense textile grid in SP-5 created a uniform "bridging effect" that arrested crack propagation, which allows the joint to reach the highest capacity (Triantafillou et al. 2006).

3.2 Strength Efficiency and Cost-Benefit Analysis

The envelope curve data (Table 5) and cost analysis (Table 6) highlight a critical trade-off between immediate bond strength and overall structural economy of each retrofitting method.

Table 5: Comparison of ultimate load capacities of the specimens

Specimen	Peak Load (kN)		Strength increment (%)	
	Upward direction	Downward direction	Upward direction	Downward direction
SP-1	103	98.20	-	-
SP-2	124.11	112.30	20.50	14.36
SP-3	115.87	105.57	12.50	7.51
SP-4	128.70	118.44	24.95	20.61
SP-5	135.97	128.87	32	31.23

3.2.1 Strength Efficiency

A single layer of CFRP provided a 20.5% strength increase, outperforming the single layer of TRM (12.5%). This is because the epoxy resin provides a near-perfect rigid bond that fully mobilizes the fiber strength immediately upon loading. However, efficiency scales with TRM layers. The three-layer TRM system achieved a 32% gain, proving that the mechanical interlock of multiple grids can generate confinement pressure superior to standard CFRP by distributing tensile stresses more evenly across the composite cross-section (Zhou et al. 2019).

3.3 Cost-Benefit Analysis

The Table 6 below shows the costs of using different retrofit methods for strengthening the specimens.

Table 6: Cost comparison between CFRP and TRM layer

Specimen	Wrapping area (m^2)	Cost	
		BDT/m^2	\$/m^2
CFRP (one layer)	4.16	14201	140
TRM (one layer)	4.16	3861	37
TRM (two layer)	8.32	7722	75
TRM (three layre)	12.48	11583	110

It costs \$140/m^2 to add one layer of CFRP to the specimen and \$37/m^2 to add one layer of TRM. The cost of adding two and three layers to the specimen is \$75/m^2 and \$110/m^2, respectively. Economically, the three-layer TRM system (\$110/m²) is 21% cheaper than the single-layer CFRP system (\$140/m²) while delivering higher strength. Furthermore, CFRP systems are susceptible to interfacial degradation when exposed to moisture and lose bond strength rapidly at elevated temperatures due to epoxy softening (Shrestha et al. 2016; Yin et al. 2025). In contrast, the TRM system utilizes a fire-resistant, vapor-permeable mortar matrix that ensures better long-term compatibility with the concrete substrate (Tetta et al. 2015). Thus, multi-layer TRM offers a more sustainable and cost-effective solution for seismic retrofitting.

4. CONCLUSIONS

This study numerically investigated the structural effectiveness and economic feasibility of retrofitting non-ductile beam-column joints using CFRP and TRM. From parametric finite element analysis and cost comparison, we came to the following conclusions:

- All retrofitting schemes improved the joint's load-carrying capacity. Single-layer CFRP provided a superior immediate strength gain of 20.5% (upward) and 14.36% (downward) due to the rigid bond of the epoxy resin.
- The effectiveness of TRM improved non-linearly with additional layers. The two-layer TRM specimen theoretically surpassed the single-layer CFRP, while the three-layer specimen achieved the maximum strength gains of 32% (upward) and 31.23% (downward).
- TRM was identified as the far more efficient engineering solution. The high-performance three-layer TRM configuration (\$110/m²) is 21% cheaper than the single-layer CFRP system (\$140/m²) while delivering superior ultimate load capacity. The difference is driven by the use of affordable mortar rather than expensive epoxy resins.

Therefore, while single-layer CFRP works better than single-layer TRM, the TRM system, when used in multiple layers, is more cost-effective and better for structural integrity, making it a very good choice for strengthening weak buildings.

5. LIMITATIONS AND FUTURE SCOPE

This study relies on nonlinear numerical analysis using standard constitutive material models. Specific experimental validation of the multi-layer TRM configurations was outside the scope of this work. Consequently, these results should be interpreted as a comparative assessment of structural potential and economic feasibility. Future research should focus on physical laboratory testing to calibrate these numerical predictions.

Declaration of Use of AI: During the preparation of this work, the authors utilized Generative AI tools minimally to assist with specific editorial tasks. The application of these tools was strictly limited to grammatical sentence correction, preliminary information retrieval for literature review, and the generation of structured sentences to enhance clarity and flow. The core research methodology, finite element modeling, data analysis, and scientific conclusions were performed exclusively by the authors. The authors carefully reviewed and verified all AI-assisted content and take full responsibility for the accuracy and integrity of the final manuscript.

REFERENCES

Allam, Said M., Hazem M. F. Elbakry, and Israa S. E. Arab. 2018. "Exterior Reinforced Concrete Beam Column Joint Subjected to Monotonic Loading." *Alexandria Engineering Journal* 57(4):4133–44. doi:10.1016/J.AEJ.2018.10.015.

Al-Salloum, Y. A., N. A. Siddiqui, A. A. Abadel, S. H. Alsayed, and T. H. Almusallam. 2012. "Seismic Behavior of TRM and GFRP Upgraded RC Exterior Beam-Column Joints." Pp. 1–4 in *Proceedings of the 15th European Conference on Composite Materials*. Venice.

Ghobarah, Ahmed, and A. Said. 2002. "Shear Strengthening of Beam-Column Joints." *Engineering Structures* 24(7):881–88. doi:10.1016/S0141-0296(02)00026-3.

Golias, Emmanouil, and Chris Karayannis. 2025. "Effect of C-FRP (Carbon Fiber Reinforced Polymer) Rope and Sheet Strengthening on the Shear Behavior of RC Beam-Column Joints." *Fibers* 13(9). doi:10.3390/fib13090113.

Kaliluthin, A. K., S. Kothandaraman, and T. S. Suhail Ahamed. 2014. "A Review on Behavior of Reinforced Concrete Beam-Column Joint." *International Journal of Innovative Research in Science, Engineering and Technology* 3(4):11299–312.

Kim, Sangwoo, Wonchang Choi, and Jinsup Kim. 2025. "Performance Evaluation of Reinforced Concrete Beams with Corroded Rebar Strengthened by Carbon Fiber-Reinforced Polymer." *Polymers 2025, Vol. 17, Page 1021* 17(8):1021. doi:10.3390/POLYM17081021.

Pan, Yunfeng, Guijun Xian, and Manuel A. G. Silva. 2015. "Effects of Water Immersion on the Bond Behavior between CFRP Plates and Concrete Substrate." *Construction and Building Materials* 101:326–37. doi:10.1016/J.CONBUILDMAT.2015.10.129.

Pauline, T., G. Janardhanan, P. Sangeetha, and V. Ashok. 2022. "Retrofitting of Exterior Beam-Column Joint—a Review." Pp. 279–89 in *Sustainable Practices and Innovations in Civil Engineering*, edited by S. Naganathan, K. N. Mustapha, and T. Palanisamy. Singapore: Springer Singapore.

Said, A. M., and M. L. Nehdi. 2004. "Use of FRP for RC Frames in Seismic Zones: Part I. Evaluation of FRP Beam-Column Joint Rehabilitation Techniques." *Applied Composite Materials* 11(4):205–26. doi:10.1023/B:ACMA.0000035462.41572.7A.

Shrestha, Justin, Dawei Zhang, and Tamon Ueda. 2016. "Durability Performances of Carbon Fiber–Reinforced Polymer and Concrete-Bonded Systems under Moisture Conditions." *Journal of Composites for Construction* 20(5). doi:10.1061/(asce)cc.1943-5614.0000674.

Tetta, Zoi C., Lampros N. Koutas, and Dionysios A. Bournas. 2015. "Textile-Reinforced Mortar (TRM) versus Fiber-Reinforced Polymers (FRP) in Shear Strengthening of Concrete Beams." *Composites Part B: Engineering* 77:338–48. doi:10.1016/J.COMPOSITESB.2015.03.055.

Triantafillou, T. C., C. G. Papanicolaou, P. Zissimopoulos, and T. Laourdekis. 2006. "Concrete Confinement with Textile-Reinforced Mortar Jackets." *ACI Structural Journal* 103(1):28–37. doi:10.14359/15083.

Vijayan, Dhanasingh Sivalinga, Arvindan Sivasuriyan, Parthiban Devarajan, Anna Stefańska, Łukasz Wodzyński, and Eugeniusz Koda. 2023. "Carbon Fibre-Reinforced Polymer (CFRP) Composites in Civil Engineering Application—A Comprehensive Review." *Buildings 2023, Vol. 13, Page 1509* 13(6):1509. doi:10.3390/BUILDINGS13061509.

Wang, Fuji, Xiaonan Wang, Rui Yang, Hanqing Gao, Youliang Su, and Guangjian Bi. 2017. "Research on the Carbon Fibre-Reinforced Plastic (CFRP) Cutting Mechanism Using Macroscopic and Microscopic Numerical Simulations." *Journal of Reinforced Plastics and Composites* 36(8):555–62. doi:10.1177/0731684416684966.

Yin, Yushi, Qinhua Yang, Zhihui Zhang, Haiyang Luan, and Chen Li. 2025. "Experimental Study on the Residual Interfacial Bonding Performance between CFRPs and Concrete after High Temperatures." *Advances in Bridge Engineering* 6(1). doi:10.1186/s43251-025-00168-2.

Zhou, Fen, Huanhui Liu, Yunxing Du, Lingling Liu, Deju Zhu, and Wei Pan. 2019. "Uniaxial Tensile Behavior of Carbon Textile Reinforced Mortar." *Materials 2019, Vol. 12, Page 374* 12(3):374. doi:10.3390/MA12030374.